Communication

Sizable Concentration-Dependent Frequency Shifts in Solution NMR Using Sensitive Probes

Susie Y. Huang, Clemens Anklin, Jamie D. Walls, and Yung-Ya Lin

J. Am. Chem. Soc., **2004**, 126 (49), 15936-15937• DOI: 10.1021/ja046208s • Publication Date (Web): 19 November 2004

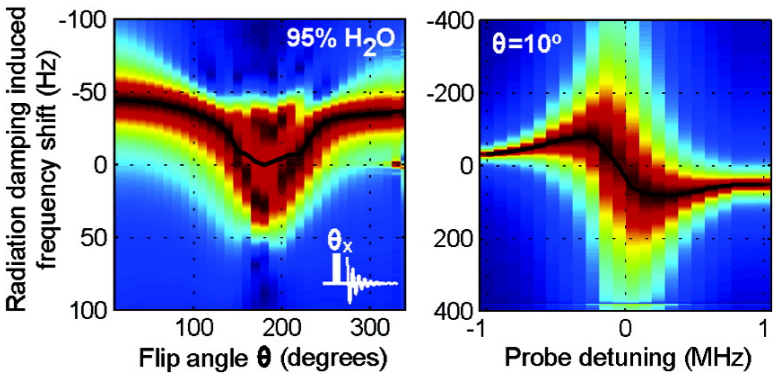

More About This Article

Additional resources and features associated with this article are available within the HTML version:

- Supporting Information
- Access to high resolution figures
- Links to articles and content related to this article
- Copyright permission to reproduce figures and/or text from this article

View the Full Text HTML

J|A|C|S
COMMUNICATIONS

Published on Web 11/19/2004

Sizable Concentration-Dependent Frequency Shifts in Solution NMR Using Sensitive Probes

Susie Y. Huang,[†] Clemens Anklin,[‡] Jamie D. Walls,[†] and Yung-Ya Lin*,[†]

Department of Chemistry and Biochemistry, University of California at Los Angeles, Los Angeles, California 90095, and Bruker Biospin Corporation, Billerica, Massachusetts 01821

Received June 27, 2004; E-mail: yylin@chem.ucla.edu

With the development of ultrasensitive probes and high-field magnets for solution NMR, striking phenomena emerge in the presence of concentrated, high-gyromagnetic ratio (γ) spin species. For example, spins residing on different molecules in solution exhibit unexpected correlations due to the distant dipolar field (DDF),[1] and solvent magnetization suppressed by a crusher gradient can revive by itself through the joint action of radiation damping and the DDF.[2] Recent observations have revealed mysterious concentration-dependent frequency shifts of up to 60 Hz for water signals detected by cryogenic probes, thwarting attempts at solvent suppression.[3] Here we report an even larger frequency shift and show that radiation damping is responsible for such unexpected shifts in the precession frequencies of bulk solvents. We warn against the potential interferences that ignorance of this effect may lead to in routine experiments. Pinpointing the physical origin of the mysterious dynamics facilitates the design of simple remedies to counteract potential interferences. The unusually large radiation damping phase angles derived from excellent fits to experimental spectra demand rethinking of the radiation damping effect, which may be more profound in modern probe circuits than had been thought.

Radiation damping ($\boldsymbol{B}_r$) is an additional magnetic field that acts back on the solvent magnetization to oppose the induced current in the receiver coil and expedites the return of the bulk magnetization back to the $+z$-axis.[4,5] The magnetic field generated by radiation damping can be approximated as[6]

$$\boldsymbol{B}_r(t) = \frac{1}{\gamma\tau_r} i m_+(t) e^{-i\psi} \qquad (1)$$

where $m_+(t) = m_x(t) + i m_y(t)$ is the net transverse magnetization normalized with respect to the equilibrium magnetization M_0. The radiation damping time constant (in SI units) is $\tau_r = 2/(\mu_0 \eta M_0 Q \gamma)$, where η is the sample filling factor and Q is the probe quality factor.[4] The phase ψ of the radiation damping field is traditionally assumed to lag behind that of $m_+(t)$ by 90°, corresponding to $\psi = 0°$. In practice, however, experiments reveal that the radiation damping phase may deviate significantly from $\psi = 0°$ if the circuit is not tuned precisely to the sample or if the construction of the probe is not ideal,[6] thus creating a dynamical shift in the precession frequency of the transverse magnetization.

For experiments using high-Q probes, the instantaneous radiation damping induced frequency shift $\omega(t)$ greatly exceeds that caused by other sources, including the DDF.[7] $\omega(t)$ (in rad/s) depends on τ_r, the longitudinal magnetization $m_z(t)$, and ψ according to:[6]

$$\omega(t) = \left(\frac{\sin\psi}{\tau_r}\right) m_z(t) \qquad (2)$$

The frequency shift $\bar{\omega}$ estimated from a Fourier-transformed spectrum is the weighted average of the instantaneous frequency shift $\omega(t)$ over the acquisition period. Figure 1 shows how $\bar{\omega}$ (dark line) varies experimentally with initial m_z and tuning conditions in 95% H_2O/5% CH_2Cl_2 acquired on an inverse probe (Figure 1a−c) and a cryoprobe (Figure 1d−f) at 600 MHz. For a given set of tuning and matching conditions, τ_r and ψ are fixed, and $\omega(t)$ only depends on $m_z(t)$. From eq 2, it then follows that $\bar{\omega} = 0$ for data corresponding to evolution under radiation damping starting with $m_z = -1$. This is seen in Figure 1, where $\bar{\omega}$ is symmetric about an initial flip angle of 180° (deviations from perfect symmetry may be attributed to RF inhomogeneity or flip-angle errors) and is greatest for $m_z \approx +1$. The CH_2Cl_2 reference peak (not shown here) is +420 Hz from the water resonance and remains unchanged, as the radiation damping field induced by water is highly selective.

Figure 2 shows the dependence of $\bar{\omega}$ on probe tuning conditions. Detuning the probe increases τ_r, which narrows the line widths of the Fourier-transformed spectra and decreases $\omega(t)$ (eq 2). Probe detuning also increases ψ, which tends to counteract the effect of τ_r by increasing $\omega(t)$. Consequently, the resulting radiation damping induced frequency shift $\bar{\omega}$ as a function of probe detuning exhibits extrema, the positions of which depend on the unique probe design. For the inverse probe, $\bar{\omega}$ spans a range from −10 Hz to +20 Hz (Figure 2a), while a much larger range is found for the cryoprobe, from −81 Hz to +83 Hz (Figure 2b). The simulated spectra shown in Figure 2c are obtained by numerically solving the Bloch equations with τ_r and ψ estimated from the experimental data in Figure 2b by nonlinear regression. Comparison of Figure 2b,c reveals excellent agreement between theory and experiments.

Taking into account the dependence of $\omega(t)$ on $m_z(t)$ resolves mysteries surrounding common practice in solvent presaturation. For example, a well-known but poorly understood phenomenon in presaturation is the need to optimize the irradiation frequency of the saturating B_1 field by trial and error.[8] For successful presaturation, the B_1 field must be applied at the solvent frequency corresponding to $\omega(t) = 0$, as the initial precession of the solvent magnetization about the effective B_1 field will quickly average out $m_z(t)$ in time, leading the precession frequency to converge to that corresponding to $\omega(t) = 0$ even if $\psi \neq 0°$. For $\psi \neq 0°$, the observed solvent precession frequency differs from the irradiation frequency needed for successful presaturation. Consequently, simply irradiating at the observed solvent frequency may not provide adequate suppression if $\psi \neq 0°$ (Figure 3a). Instead, the irradiation frequency corresponding to $\omega(t) = 0$ can be found empirically by trial and error to optimize solvent suppression (Figure 3b). Alternatively, by mapping out the profile shown in Figure 2a to find the tuning conditions such that $\psi = 0°$, the observed frequency will be rendered independent of $m_z(t)$. Direct irradiation at the observed solvent frequency under these conditions then provides optimal presaturation (Figure 3c). This confirms that frequency shifts induced

[†] University of California at Los Angeles.
[‡] Bruker Biospin Corporation.

10.1021/ja046208s CCC: $27.50

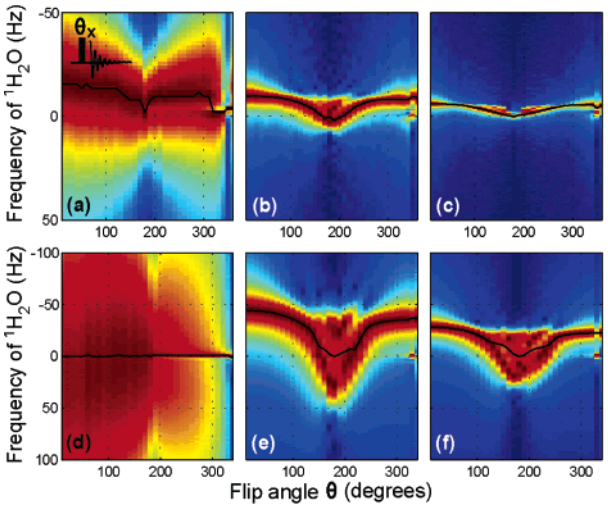

Figure 1. Contour plots of stacked 95% H_2O/5% CH_2Cl_2 ^1H frequency spectra (normalized to the peak) at 300 K as a function of pulse flip angle θ_x. Experiments were performed on a 600 MHz Bruker AVANCE spectrometer for both a triple resonance broadband inverse probe (a−c) and a cryoprobe (d−f). A sealed capillary tube containing D_2O was placed in the sample for field-frequency lock. In all experiments, the probe was matched to the sample. (a) Tuned inverse probe. (b) Inverse probe detuned by +2.9 MHz. (c) Inverse probe detuned by +8 MHz. (d) Tuned cryoprobe. (e) Cryoprobe detuned by −0.5 MHz. (f) Cryoprobe detuned by −1 MHz.

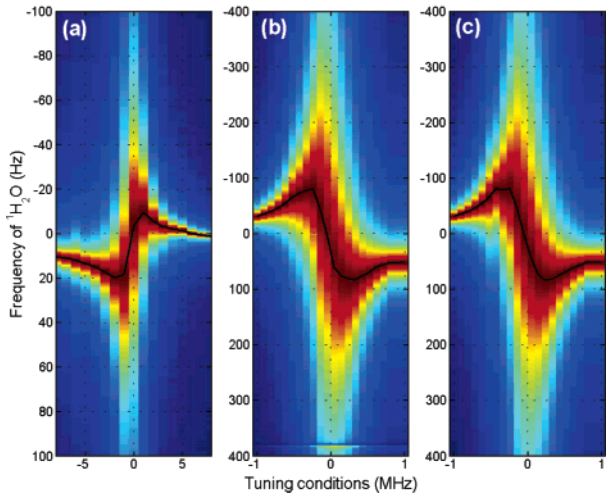

Figure 2. Contour plots of stacked 95% H_2O/5% CH_2Cl_2 ^1H frequency spectra (normalized to the peak) at 300 K as a function of probe detuning. Spectra were acquired after applying a 10° pulse to the sample. (a) Inverse probe with tuning conditions varied from −8 MHz below to +8 MHz above resonance. (b) Cryoprobe with tuning conditions varied from −1 MHz below to +1 MHz above resonance. (c) Simulations with parameters τ_r and ψ obtained from best fits to data in (b).

by radiation damping are responsible for the empirical practice of adjusting the B_1 irradiation frequency to optimize presaturation.

The radiation damping induced frequency shift will become larger with the advent of higher fields and more sensitive probes. To avoid such spurious shifts when observing abundant spin species, radiation damping may be counteracted by incorporating active electronic feedback[9] or variable *Q*-switching[10] into current probe designs. A simpler way to circumvent complications due to radiation damping is to set the irradiation frequency in presaturation to the frequency of the residual solvent magnetization signal following suppression by other means, e.g., WATERGATE.

Advantages of the radiation damping induced frequency shift include allowing the spins to reveal the true optimal probe tuning conditions, as $\psi = 0°$ only when the probe is perfectly tuned. Under

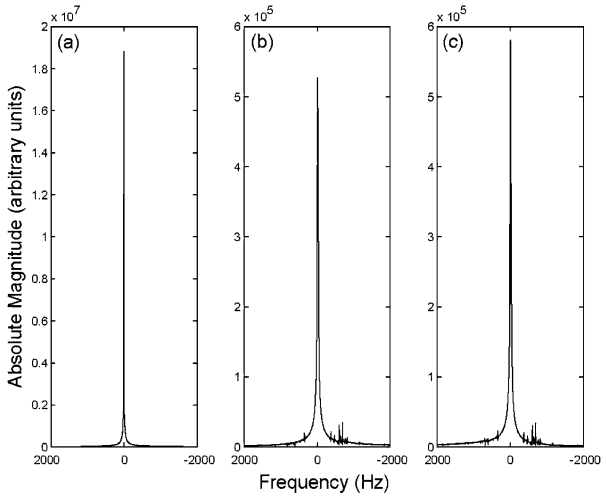

Figure 3. Presaturation spectra performed on a sample of 2 mM sucrose, 0.5 mM DSS, 2 mM NaN_3, 10% D_2O, and 90% H_2O at 300 K using an RF amplitude of 27 Hz. All frequency spectra are centered on the water peak. (a) Irradiation at the apparent water ^1H resonance frequency on an optimally tuned probe. (b) Irradiation at +8 Hz above the apparent water resonance frequency under the same tuning conditions as in (a). Note the change in vertical scale. (c) Irradiation at the apparent water resonance frequency after detuning the probe by −0.4 MHz, which shifts the center frequency of water by +8 Hz.

such optimal tuning conditions, experiments suggest that the signal-to-noise ratio may be improved by up to 20% compared to the assumed best tuning conditions indicated by the oscilloscope or tuning device. The presence of a large radiation damping induced frequency shift can also provide valuable insight into the real-time evolution of $m_z(t)$, which will be detailed elsewhere. The ψ estimated from fitting the experimental spectra in Figures 1 and 2 can be very large (up to ±75°; see also Supporting Information). The exceedingly good match between experiments and the fitted spectra suggests that the estimated ψ may be physically valid, which merits further investigation.

Acknowledgment. We thank the reviewers for helpful suggestions and Rainer Haessner and M. Jane Strouse for drawing our attention to the concentration-dependent frequency shift. This work was supported by the Camille and Henry Dreyfus Foundation, Research Corporation, UCLA Career Development Program, NSF Grants CHE-0116853 and CHE-0349362, and NSF Graduate Research Fellowship (S.Y.H.).

Supporting Information Available: Simulation data and fitting parameters for Figures 1 and 2. This material is available free of charge via the Internet at http://pubs.acs.org.

References

(1) (a) Warren, W. S.; Richter, W.; Andreotti, A. H.; Farmer, B. T., II. *Science* **1993**, *262*, 2005. (b) Levitt, M. H. *Concepts Magn. Reson.* **1996**, *8*, 77.
(2) Lin, Y.-Y.; Lisitza, N.; Ahn, S.; Warren, W. S. *Science* **2000**, *290*, 118.
(3) Haessner, R. Technische Universität München, Organisch-Chemisches Institut, Garching, Germany. Personal communication, 2002.
(4) Bloembergen, N.; Pound, R. V. *Phys. Rev.* **1954**, *95*, 8.
(5) Augustine, M. P. *Prog. Nucl. Magn. Reson. Spectrosc.* **2002**, *40*, 111.
(6) (a) Vlassenbroek, A.; Jeener, J.; Broekaert, P. *J. Chem. Phys.* **1995**, *103*, 5886. (b) Barjat, H.; Chadwick, G. P.; Morris, G. A.; Swanson, A. G. *J. Magn. Reson. A* **1995**, *117*, 109.
(7) Edzes, H. T. *J. Magn. Reson.* **1990**, *86*, 293.
(8) Cavanagh, J.; Fairbrother, W. J.; Palmer, A. G., III; Skelton, N. J. *Protein NMR Spectroscopy: Principles and Practice*; Academic Press: San Diego, CA, 1996.
(9) (a) Broekaert, P.; Jeener, J. *J. Magn. Reson. A* **1995**, *113*, 60. (b) Louis-Joseph, A.; Abergel, D.; Lallemand, J.-Y. *J. Biomol. NMR* **1995**, *5*, 212.
(10) (a) Maas, W. E.; Laukien, F. H.; Cory, D. G. *J. Magn. Reson. A* **1995**, *113*, 274. (b) Anklin, C.; Rindlisbacher, M.; Otting, G.; Laukien, F. H. *J. Magn. Reson. B* **1995**, *106*, 199.

JA046208S